



Istituto Nazionale di Fisica Nucleare  
SEZIONE DI TORINO



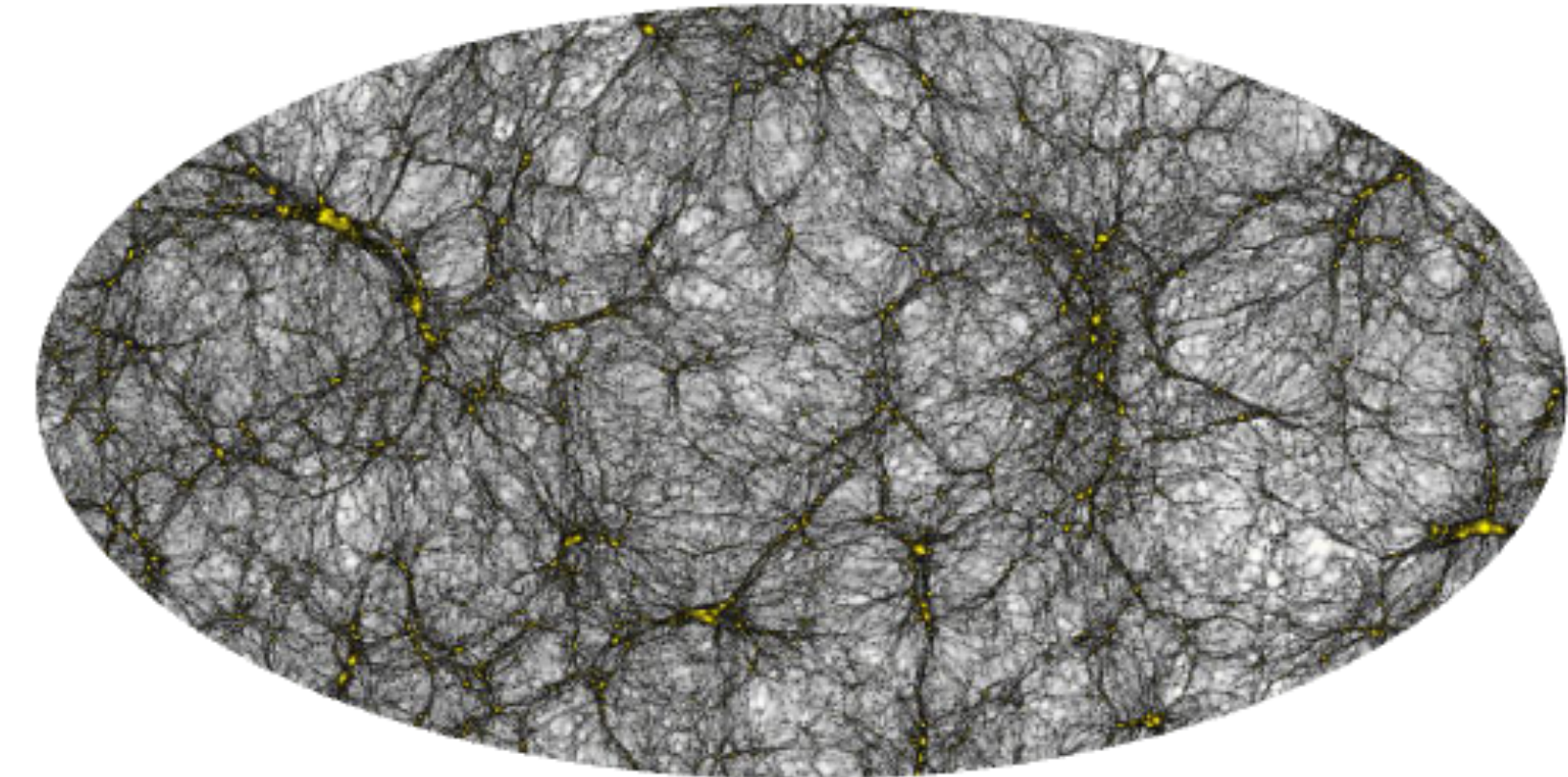
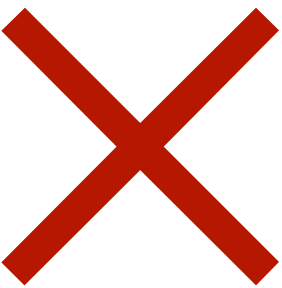
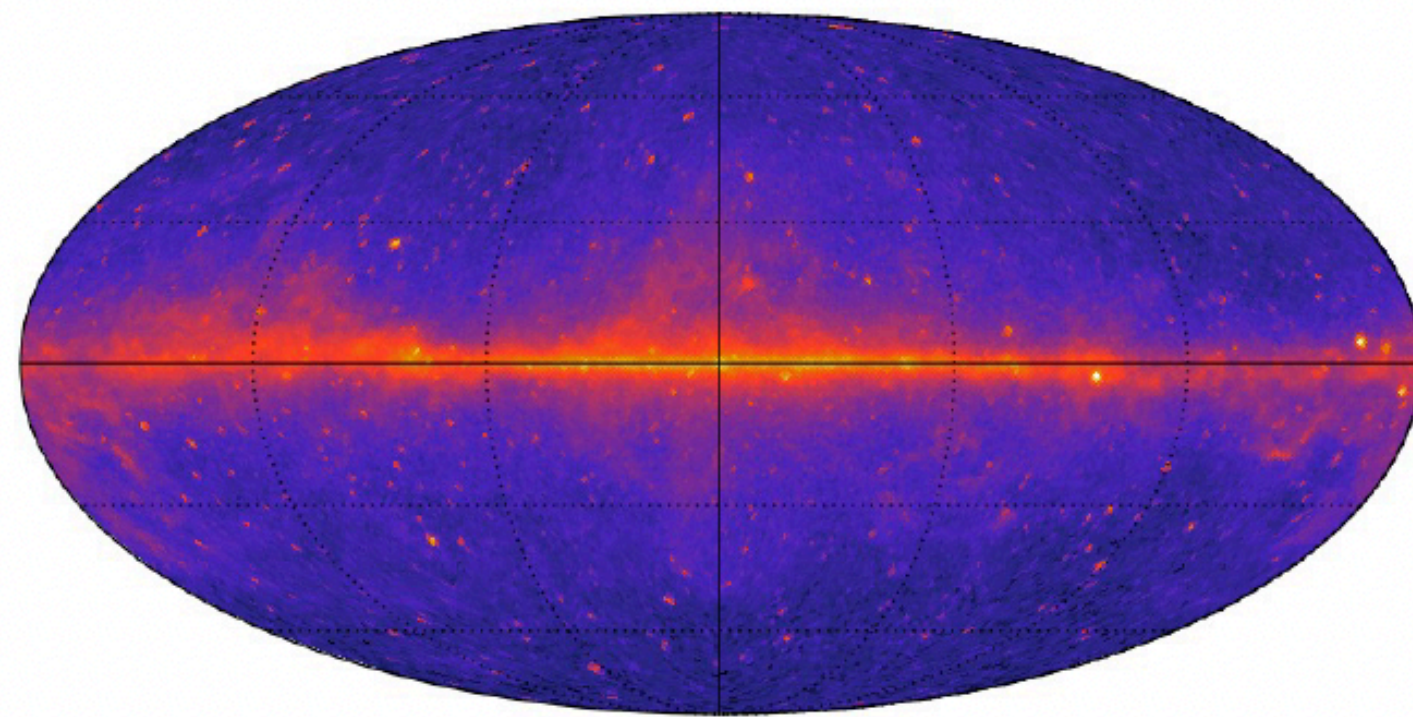
# Shear $\times$ Gamma

**Cross-correlating the Unresolved Gamma-Ray Background with Weak Lensing.**

arXiv:2501.10506

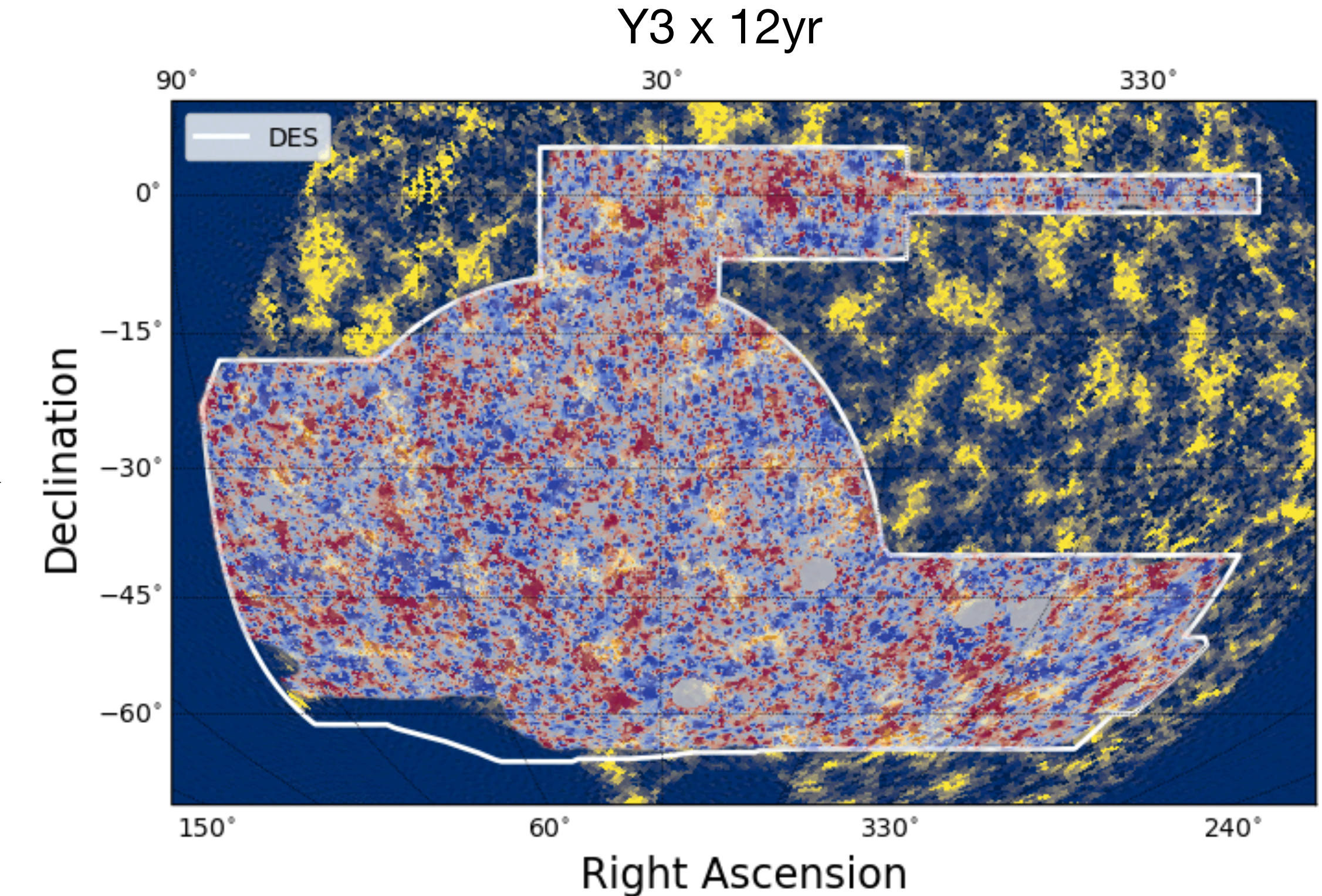
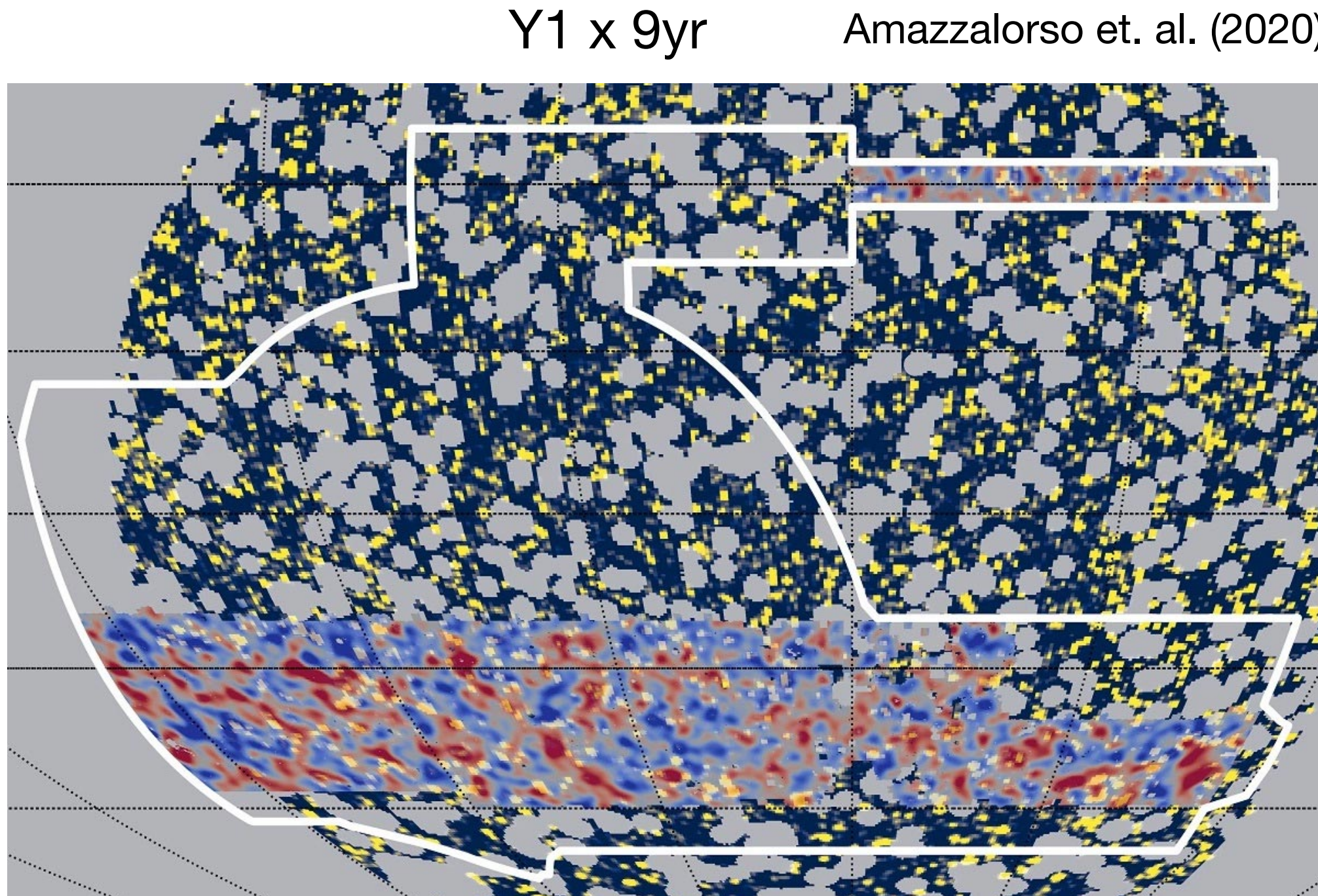
**Bhashin Thakore, 20/06/2025 (in collaboration with M. Negro, M. Regis, D. Gruen, S. Camera, N. Fornengo, A. Roodman, A. Cuoco, A. Porredon, and T. Schutt)**

# Tomographic Approaches for WIMP Search



- The fluctuations in the gamma-ray field need to be statistically correlated to the DM distribution in the universe (i.e. the DM fluctuations on top of a smooth Universe).
- Since dark matter is responsible for the weak lensing effect observed in distant source galaxies, any potential annihilation or decay from DM particles would be correlated with the lensing effect.
- The energy, redshift, and scale dependence of the cross-correlations have the potential to distinguish astrophysical signals from self-annihilating dark matter signals.

# DES Y1 x Fermi 9-yr (2020) v/s DES Y3 x Fermi 12-yr (2024)



D. Gruen/SLAC/Stanford; C. Chang/University of Chicago; A. Drlica-Wagner/Fermilab

# 2-pt Correlation Estimator

$$\Xi^{ar}(\theta) = \Xi_{\Delta\theta_h, \Delta E_a, \Delta z_r}^{\text{signal}} - \Xi_{\Delta\theta_h, \Delta E_a, \Delta z_r}^{\text{random}} = \frac{\sum_{i,j} e_{ij,t}^r I_j^a}{R \sum_{i,j} I_j^a} - \frac{\sum_{i,j} e_{ij,t}^r I_{j,\text{random}}^a}{R \sum_{i,j} I_{j,\text{random}}^a}$$

Angular bin    Energy bin    Redshift bin

Tangential ellipticity of source galaxy  $i$ , in redshift bin  $r$ , relative to pixel  $j$

Photon intensity flux in energy bin  $a$ , relative to pixel  $j$

Summation over the DES source galaxies and unmasked gamma-ray pixels

Random term, subtracted from the signal to reduce additive shear systematic effects, random very-large-scale structures or chance shear alignments relative to the mask (affecting the variance).

# Covariance

$$\hat{\Gamma}_{arl,bsl'} = \frac{\delta_{ll'}^K}{(2l+1)\Delta lf_{\text{sky}}} \left[ \underline{C_l^{ar} C_{l'}^{bs}} + (\underline{C_{l'}^{rs}} + \underline{\mathcal{N}^{rs}})(\underline{C_l^{ab}} + \underline{\mathcal{N}^{ab}}) \right]$$

*r, s: redshift bins*  
*a, b: energy bins*

Theoretical Estimate

2000 Mocks

$\hat{\Gamma}_{arl,bsl'} = \frac{\delta_{ll'}^K}{(2l+1)\Delta lf_{\text{sky}}} \left[ \underline{C_l^{ar} C_{l'}^{bs}} + (\underline{C_{l'}^{rs}} + \underline{\mathcal{N}^{rs}})(\underline{C_l^{ab}} + \underline{\mathcal{N}^{ab}}) \right]$

$r, s: \text{redshift bins}$

$a, b: \text{energy bins}$

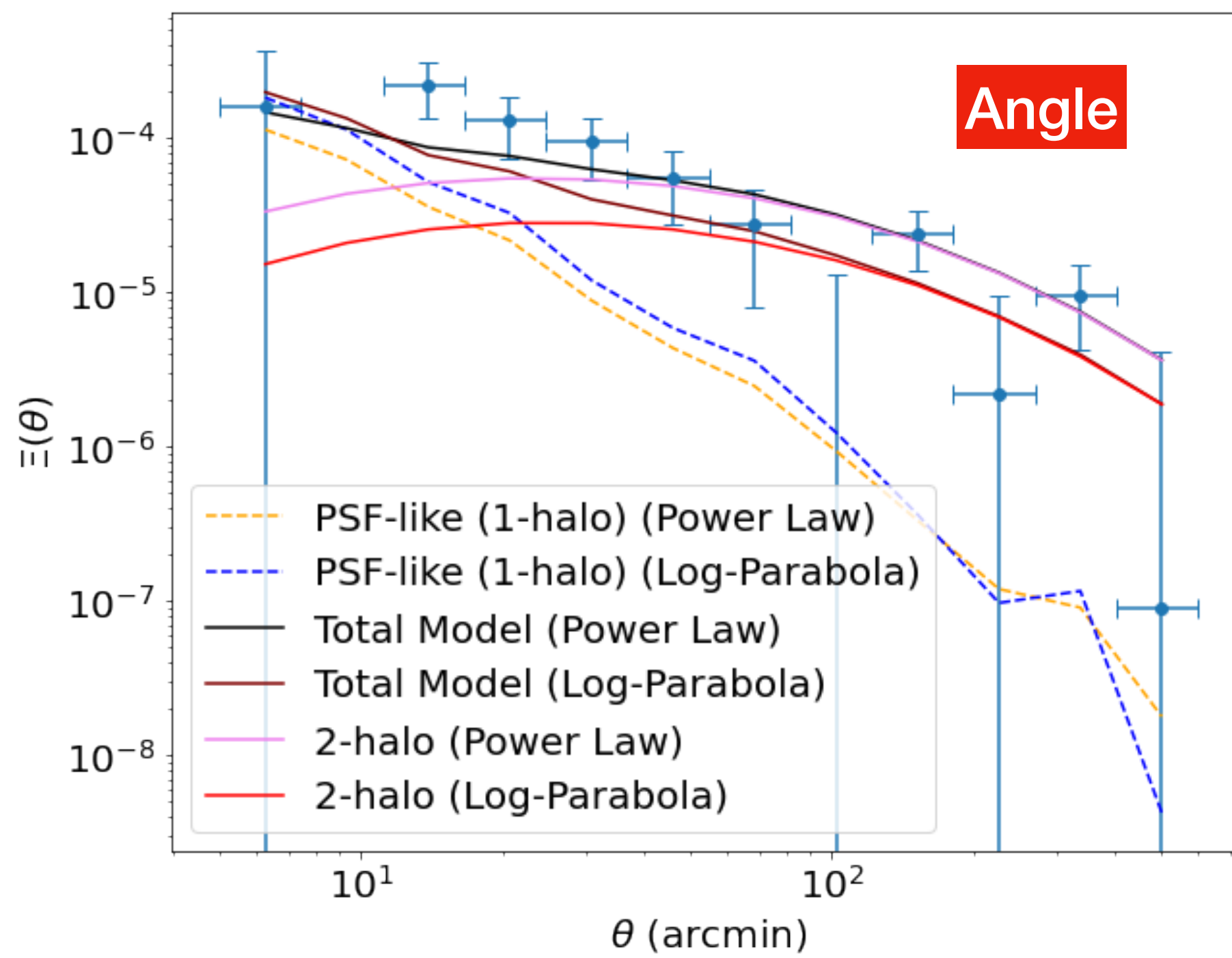
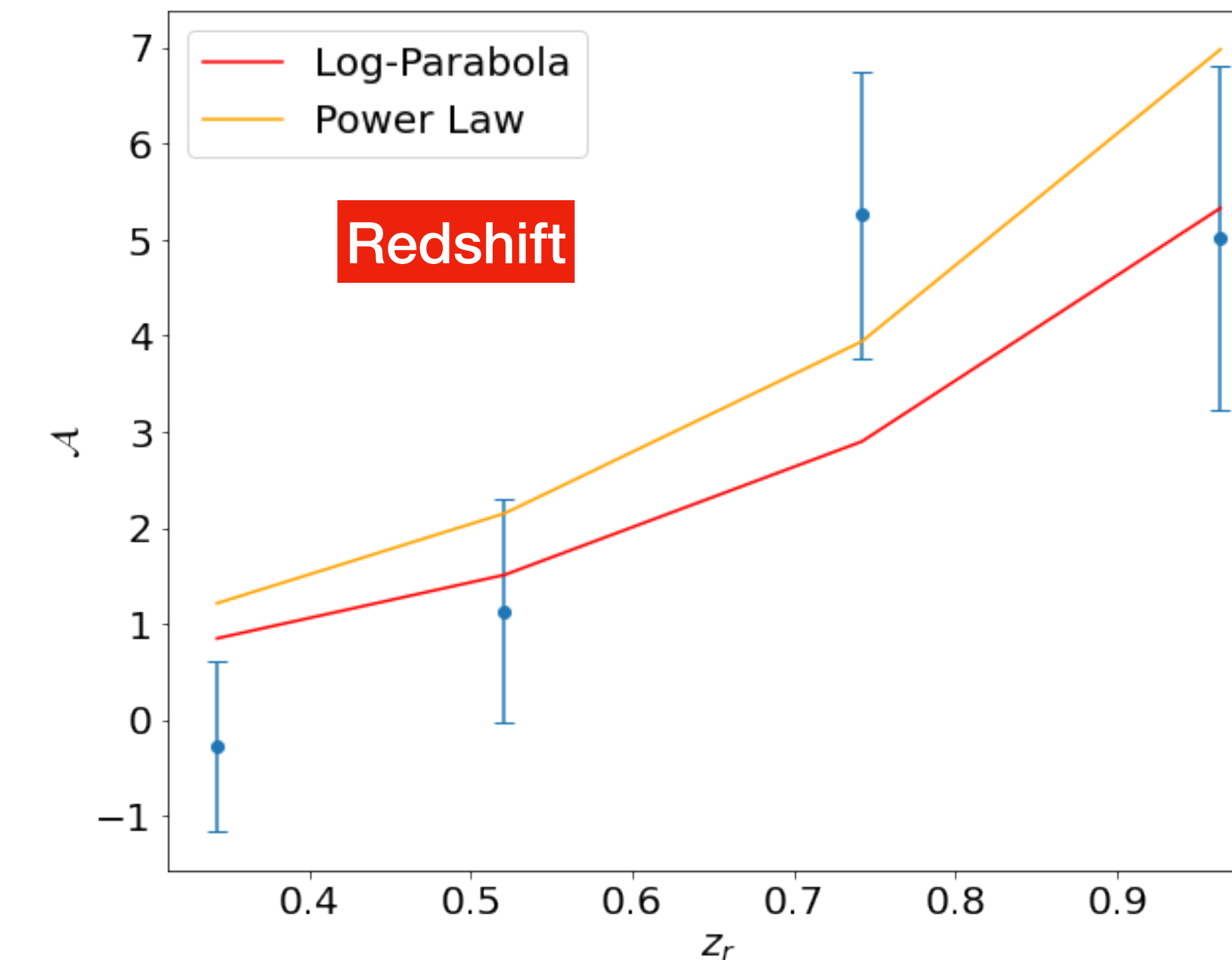
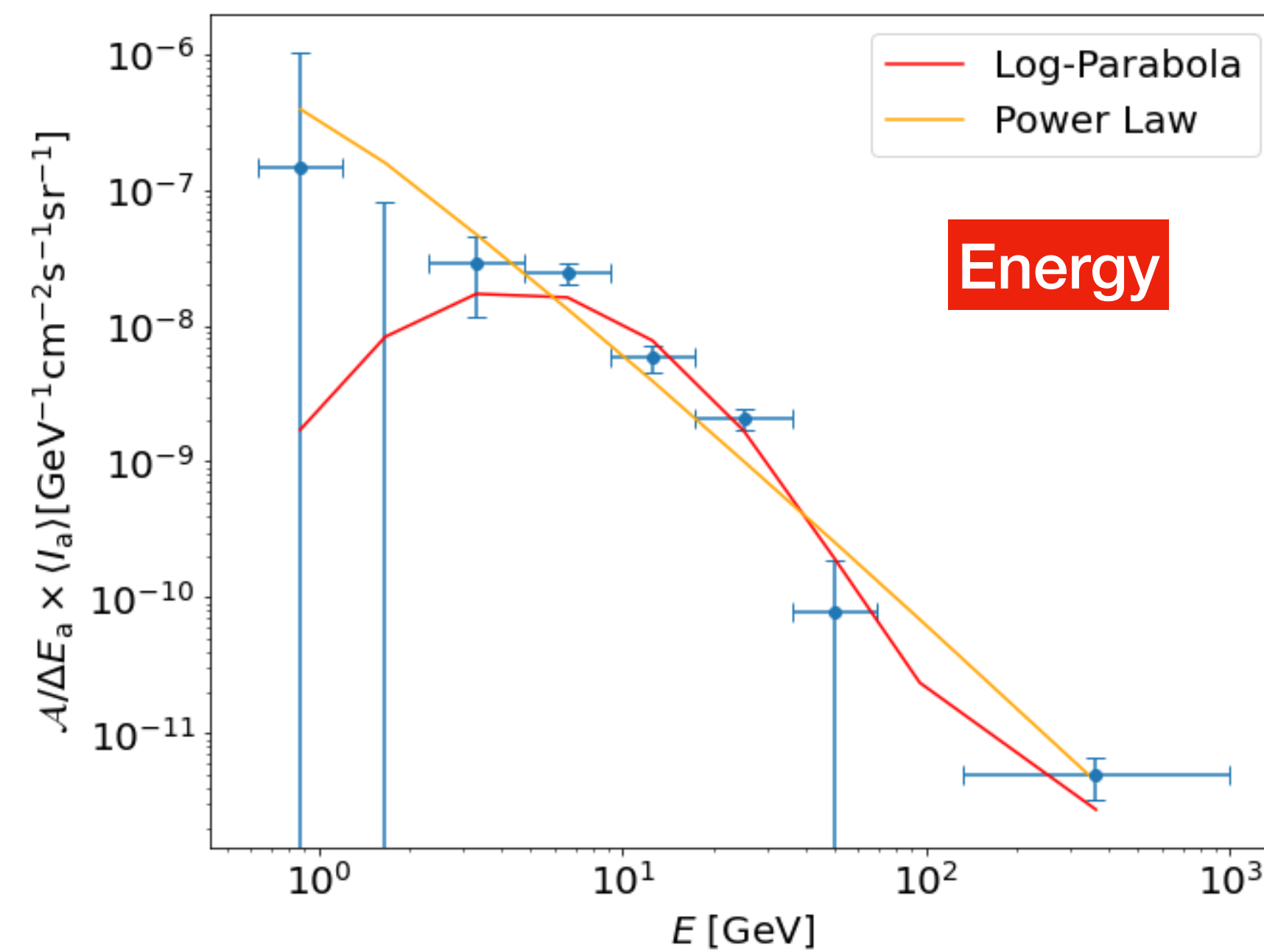
Hartlap factor =  $(N_s - N_b - 2)/(N_s - 1) \sim 0.78$

# The Phenomenological Models

- The considerations of a potential cross-correlation signal were based on two phenomenological models - the power law and the log-parabolic models.

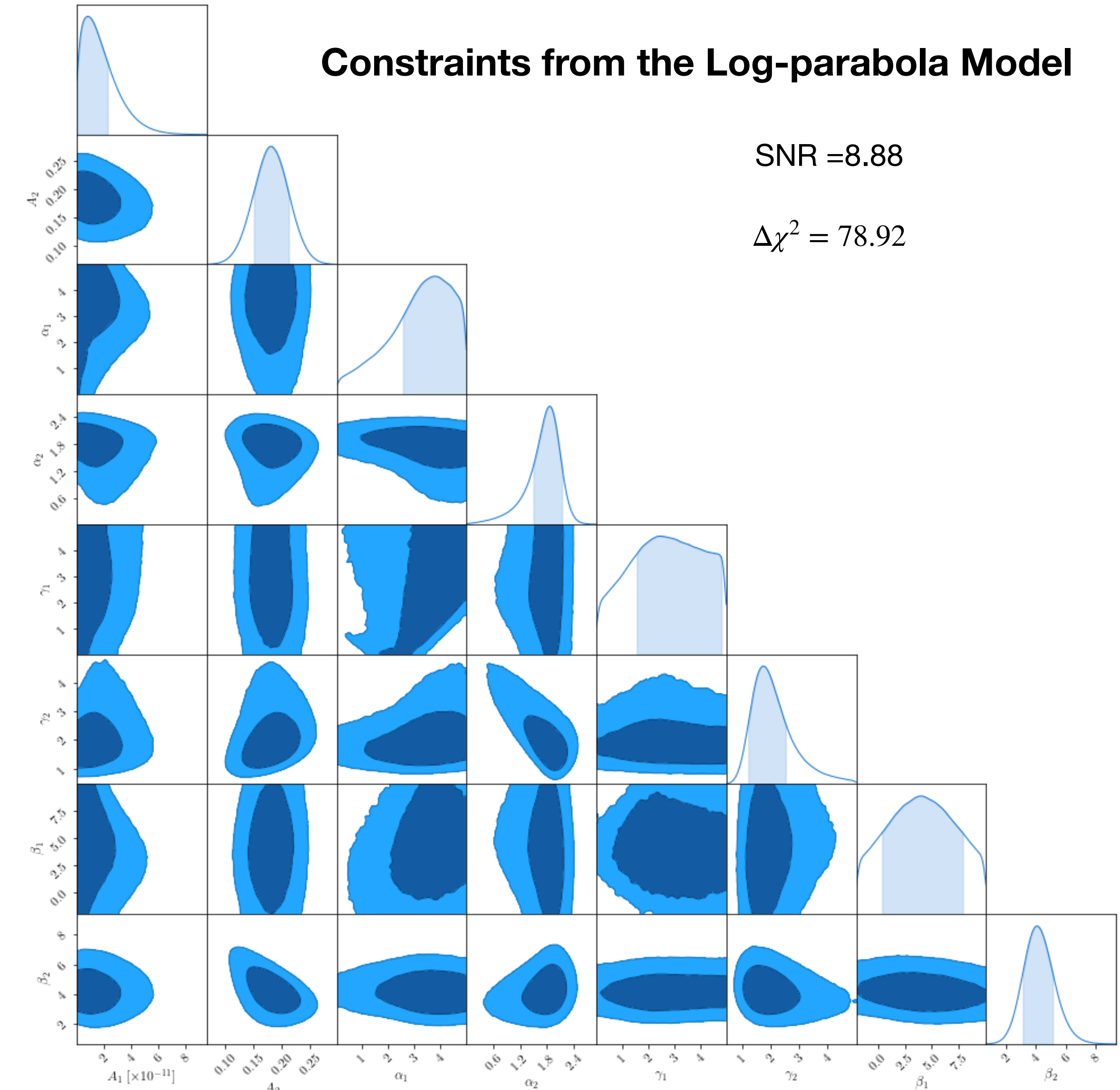
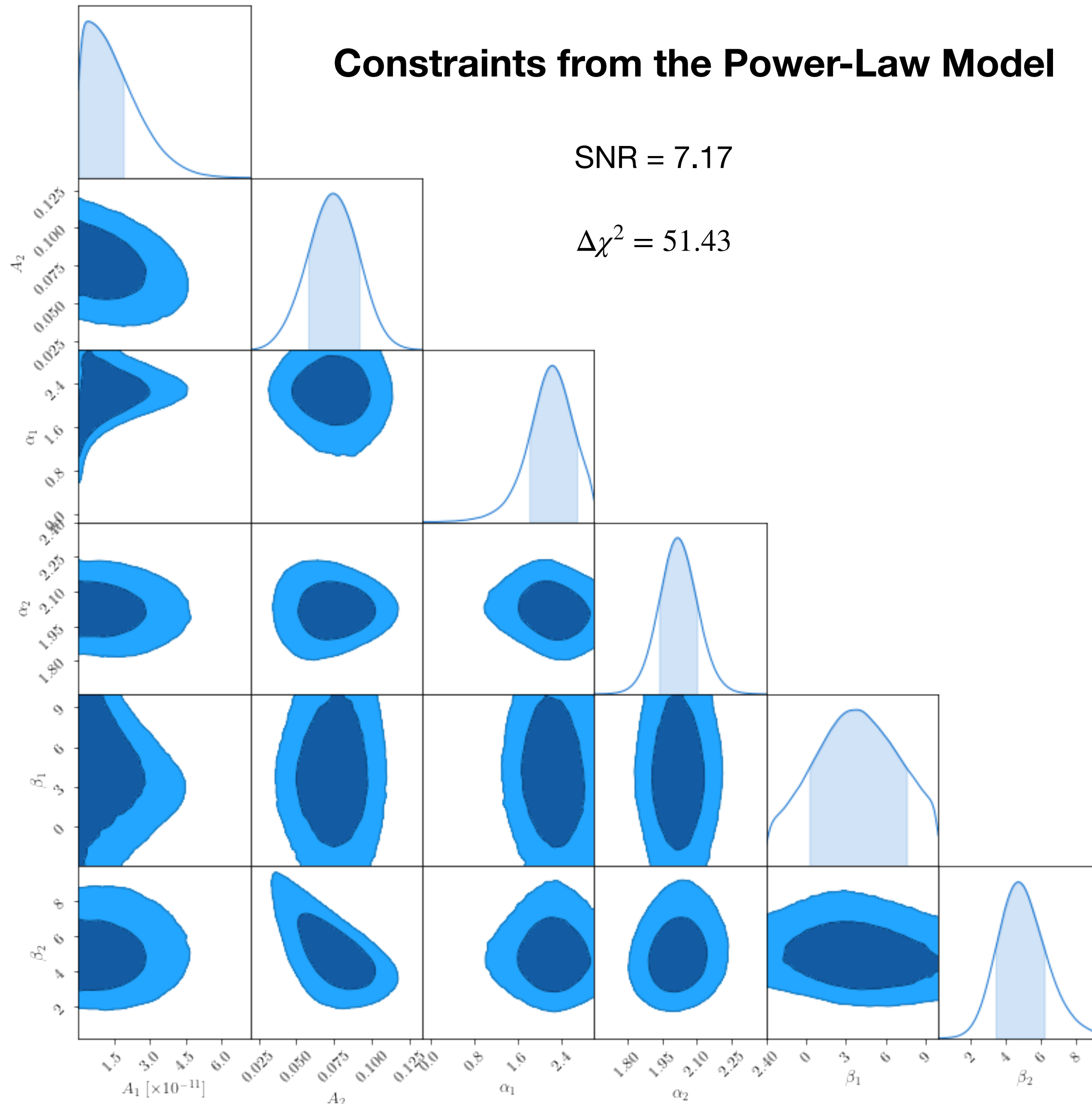
$$\Xi(\theta)_{\text{PL}} = A_1 \times \left(\frac{E_a}{E_p}\right)^{-\alpha_1} \times \left(\frac{1+z_r}{1+z_p}\right)^{\beta_1} \times \hat{\Xi}_{1-\text{halo}}^a(\theta) + A_2 \times \left(\frac{E_a}{E_p}\right)^{-\alpha_2} \times \left(\frac{1+z_r}{1+z_p}\right)^{\beta_2} \times \hat{\Xi}_{2-\text{halo}}^{ar}(\theta)$$

$$\Xi(\theta)_{\text{LP}} = A_1 \times \left(\frac{E_a}{E_p}\right)^{-\alpha_1 - \gamma_1 \log_{10} \frac{E_a}{E_p}} \times \left(\frac{1+z_r}{1+z_p}\right)^{\beta_1} \times \hat{\Xi}_{1-\text{halo}}^a(\theta) + A_2 \times \left(\frac{E_a}{E_p}\right)^{-\alpha_2 - \gamma_2 \log_{10} \frac{E_a}{E_p}} \times \left(\frac{1+z_r}{1+z_p}\right)^{\beta_2} \times \hat{\Xi}_{2-\text{halo}}^{ar}(\theta)$$



	Data set						
	Full	Low- $z$	High- $z$	Low- $E$	High- $E$	Small- $\theta$	Large- $\theta$
$\Delta\chi^2_{\text{lp}}$	78.9	3.40	75.3	23.3	55.4	5.82	73.7
SNR <sub>lp</sub>	8.88	2.45	8.70	4.89	7.49	2.42	8.58
$\Delta\chi^2_{\text{pl}}$	51.4	0.92	53.7	15.8	38.7	8.72	47.3
SNR <sub>pl</sub>	7.17	1.66	7.34	4.03	6.24	2.96	6.88

# The Phenomenological Models (Contd.)



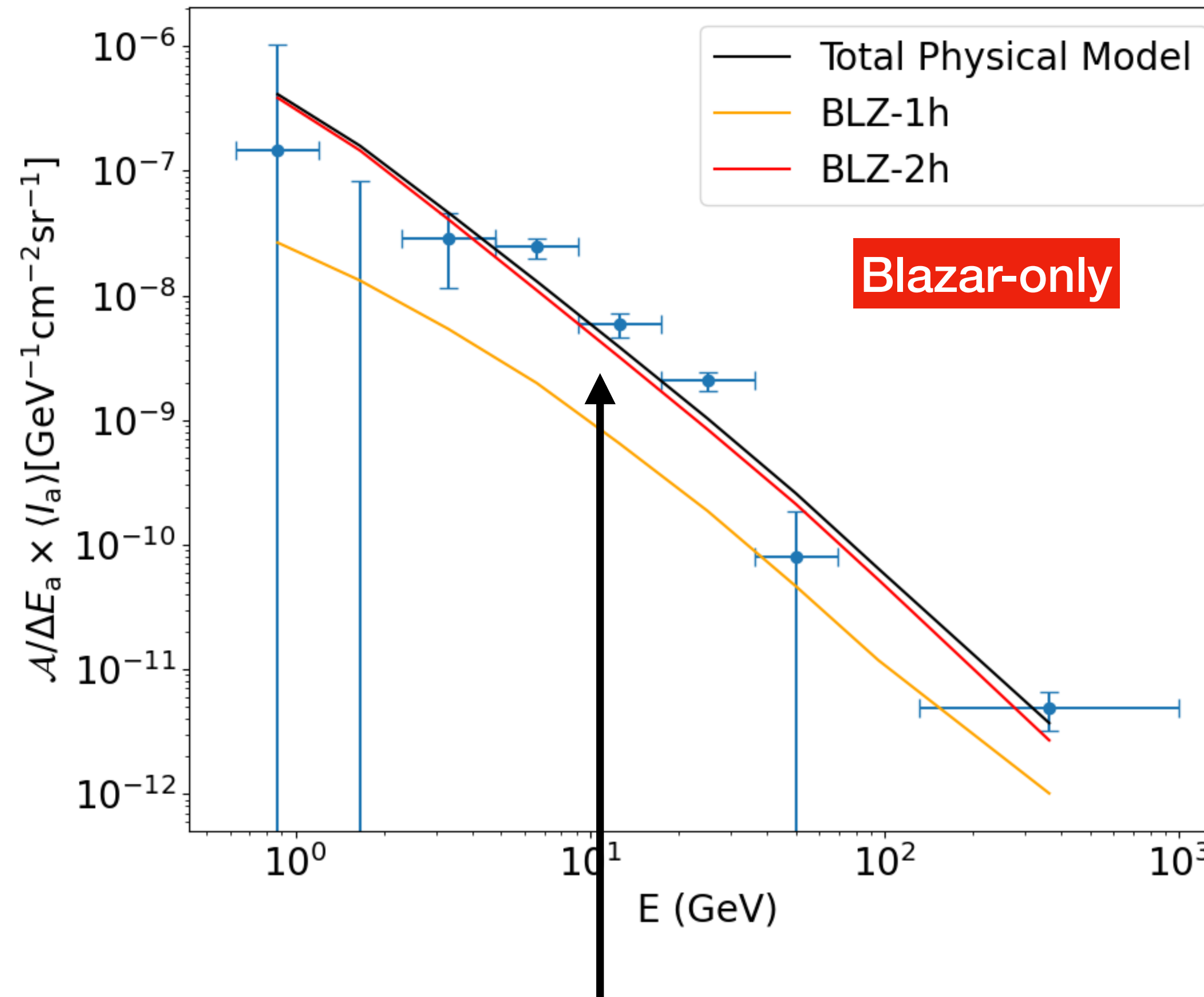
# The Physical Model

- The physical model considerations were divided into two primary categories:
  1. Astrophysics-only contributions, consisting of Blazar components.
  2. A dark matter component, consisting of a certain dark-matter model.

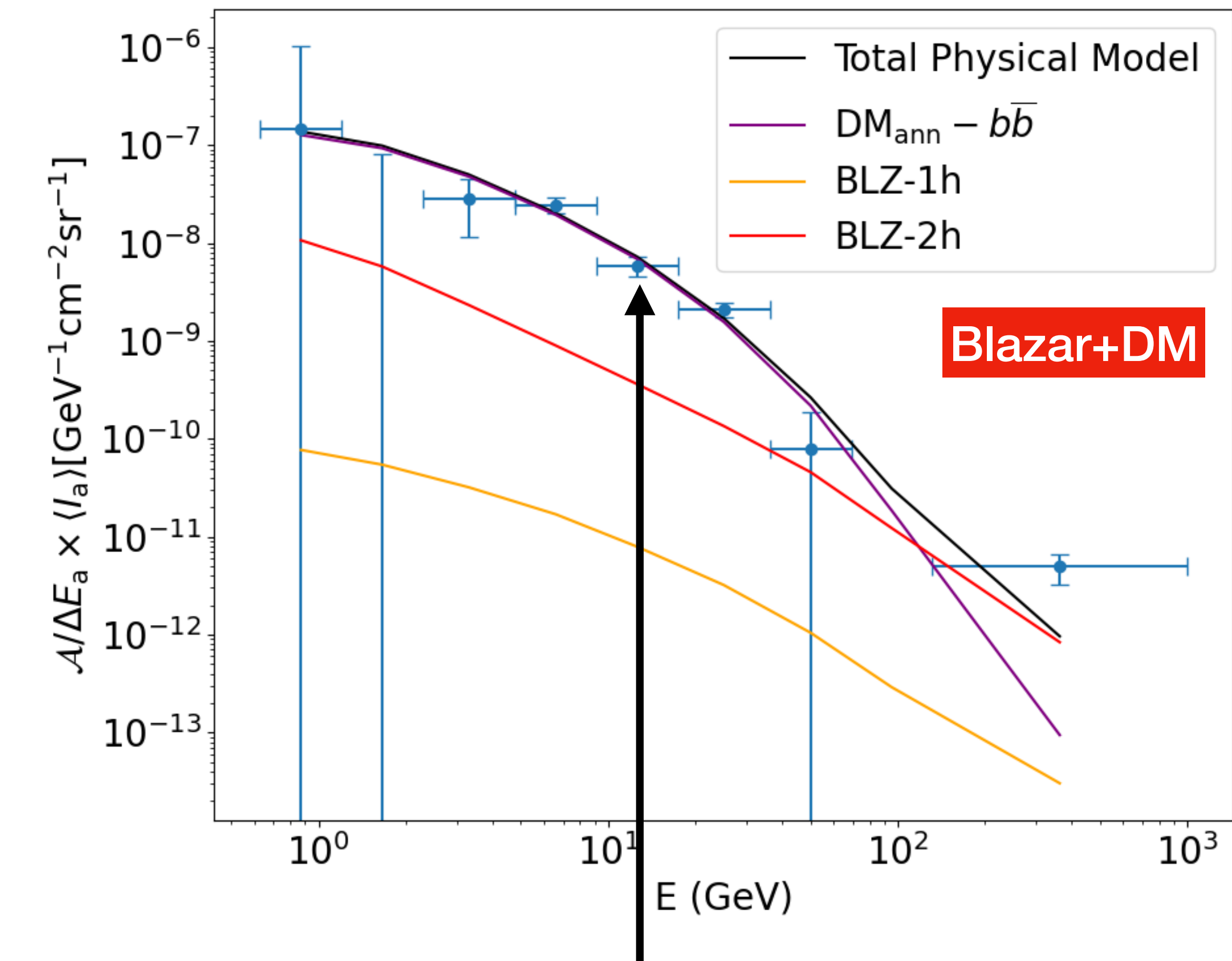
$$\Xi(\theta) = \underbrace{A_{\text{BLZ-1halo}} \times \hat{\Xi}_{\text{BLZ-1halo}}^{ar}(\theta, \mu, p_1) + A_{\text{BLZ-2halo}} \times \hat{\Xi}_{\text{BLZ-2halo}}^{ar}(\theta, \mu, p_1)}_{\text{Astrophysical components}} + \underbrace{A_{\text{DM}} \times \hat{\Xi}_{\text{DM}}^{ar}(\theta)}_{\text{Added DM component}}$$

$$\langle \sigma_{\text{ann}} \nu \rangle = 32^{+10}_{-8} \langle \sigma_{\text{ann}} \nu \rangle_{\text{th}}$$

$$m_{\text{DM}} = 363.07^{+138.10}_{-39.48} \text{ GeV}$$

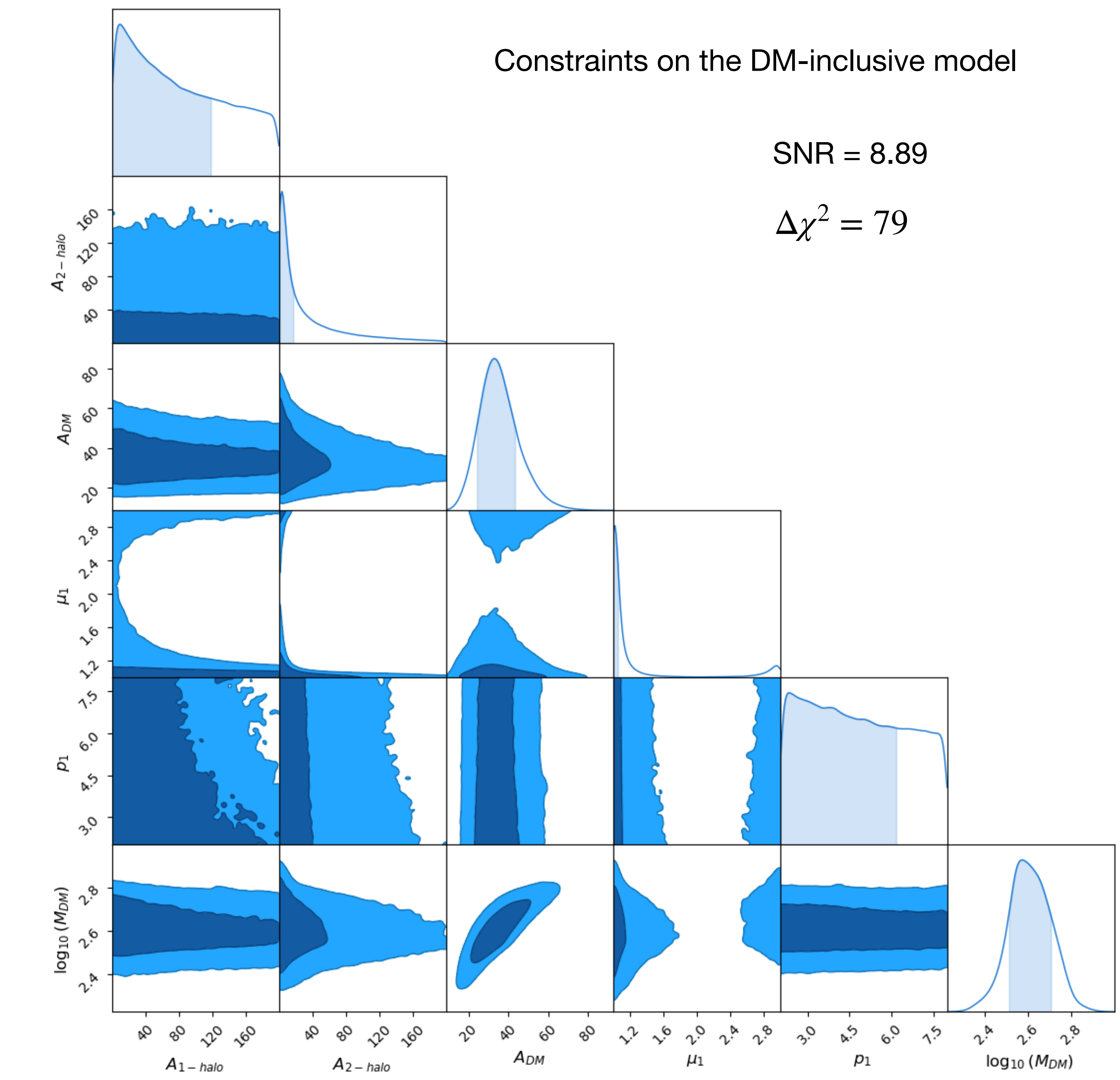
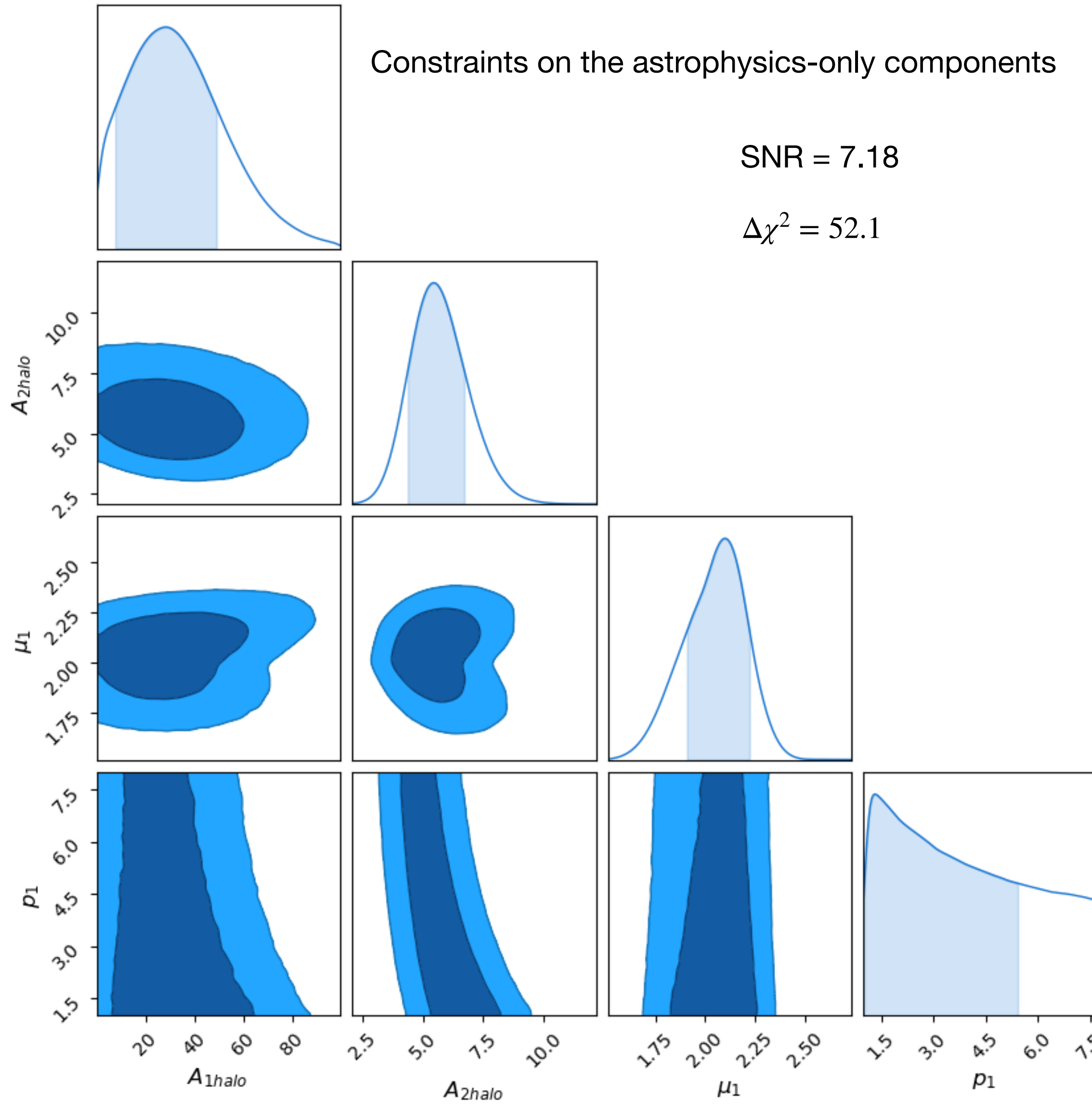


- Dominant 2-halo Blazar component.
- E-dependence not well-reproduced.



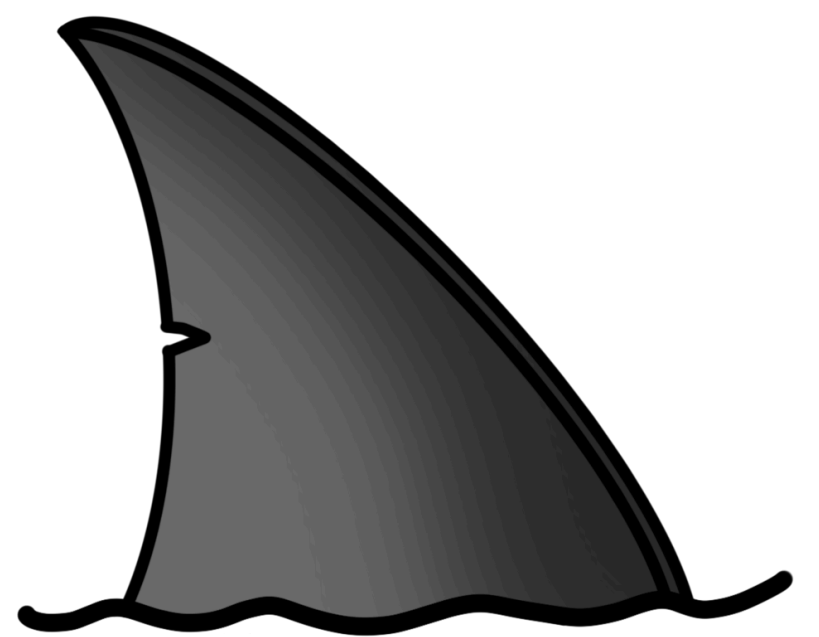
- Dominant DM component.
- E-dependence well-reproduced.
- >5-sigma preference for BLZ+DM

# The Physical Model (Contd.)



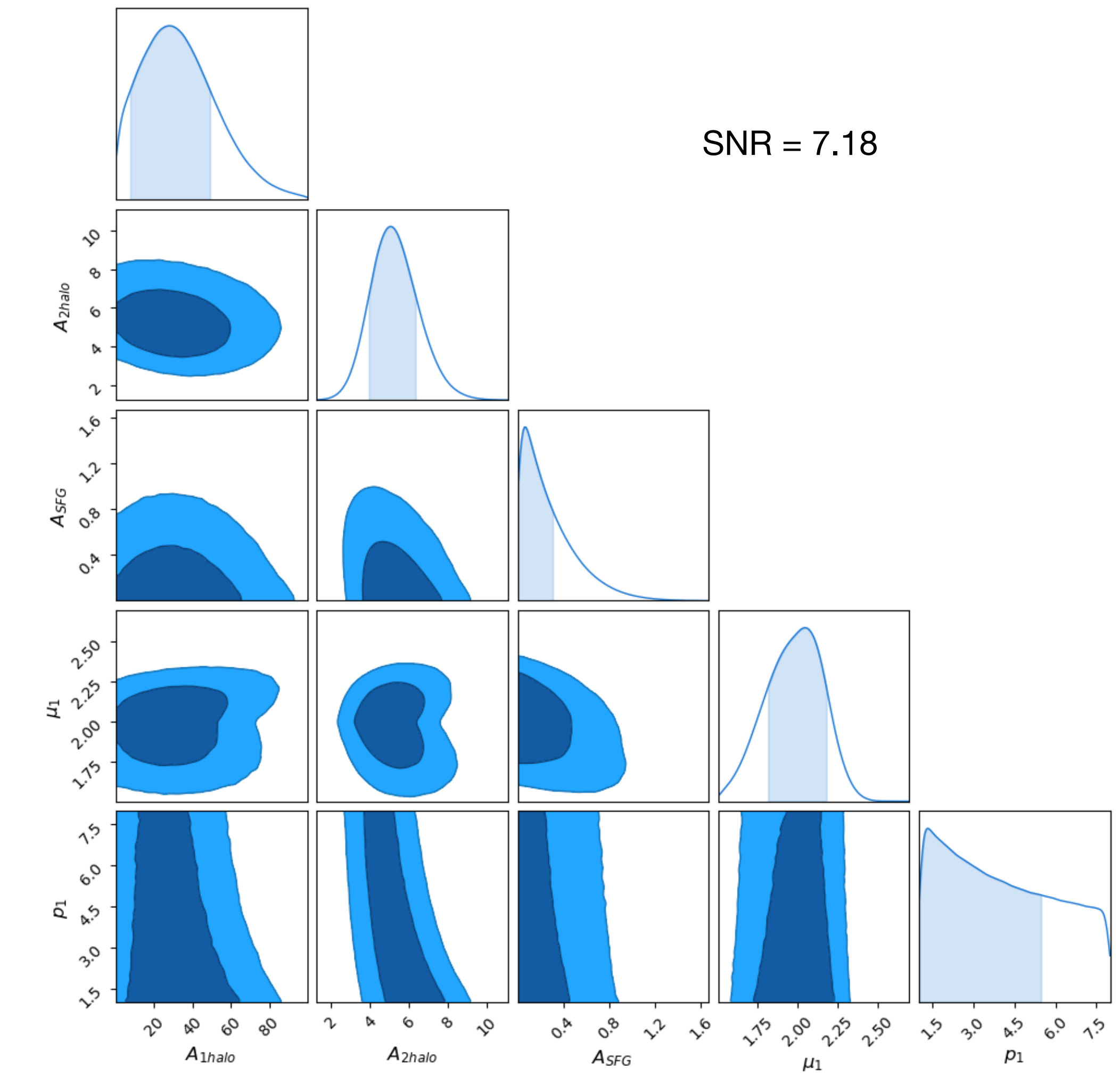
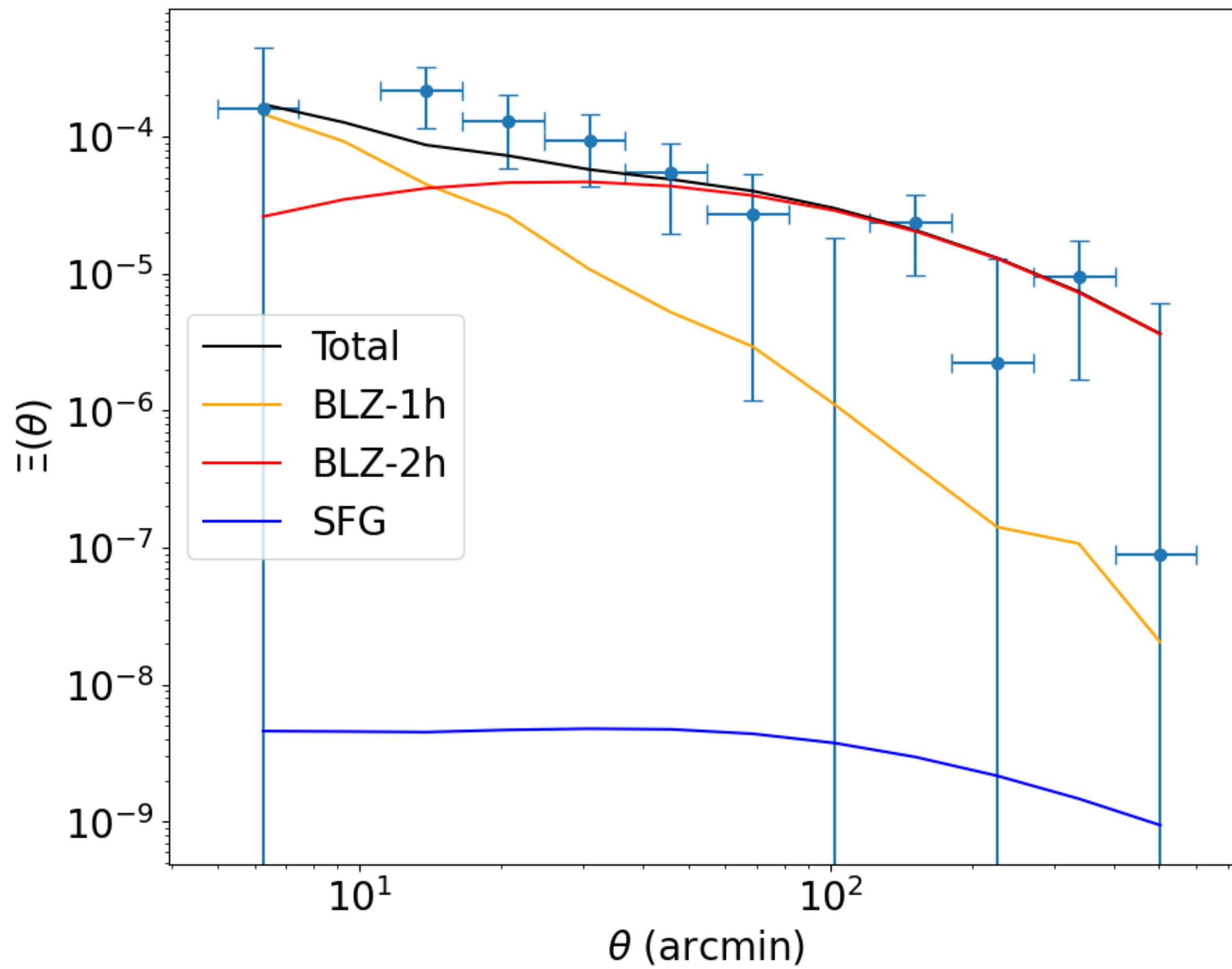
# Summary

- Cross-correlations between tracers of gravitational structure and the UGRB have the potential to separate WIMP DM signals that annihilate or decay in gamma-ray energies.
- Phenomenologically, a cross-correlation between weak lensing and the UGRB provides a significant detection of a signal, at an SNR of 8.9.
- Physically, while Blazars appear to dominate the UGRB, with the current models, they cannot explain the stronger signals obtained using the log-parabolic phenomenological model.
- A change in the way the astrophysical components are modelled as well as combining the current observations with those obtained from galaxy clustering cross-correlations could provide better constraints on both astrophysical as well as DM signals.



*Fin.*

# Blazars+SFGs



# Blazars+mAGNs

